Hindawi
International Journal of Aerospace Engineering
Volume 2018, Article ID 6081801, 10 pages
https://doi.org/10.1155/2018/6081801

*Research Article*

# Adaptive Fuzzy Sliding Mode Guidance Law considering Available Acceleration and Autopilot Dynamics

**Yulin Wang**,[1] **Shengjing Tang**,[1] **Wei Shang**,[2] **and Jie Guo**[1]

[1]*School of Aerospace Engineering, Beijing Institute of Technology, Beijing 100081, China*
[2]*System Design Institute of Hubei Aerospace Technology Academy, Hubei, 430040, China*

Correspondence should be addressed to Jie Guo; guojie1981@bit.edu.cn

Received 21 November 2017; Accepted 8 April 2018; Published 29 April 2018

Academic Editor: Vaios Lappas

Copyright © 2018 Yulin Wang et al. This is an open access article distributed under the Creative Commons Attribution License, which permits unrestricted use, distribution, and reproduction in any medium, provided the original work is properly cited.

Terminal guidance law for missiles intercepting high maneuvering targets considering the limited available acceleration and autopilot dynamics of interceptor is investigated. Conventional guidance laws based on adaptive sliding mode control theory were designed to intercept a maneuvering target. However, they demand a large acceleration for interceptor at the end of the terminal guidance, which may have acceleration saturation especially when the target acceleration is close to the available acceleration of interceptor. In this paper, a terminal guidance law considering the available acceleration and autopilot dynamics of interceptor is proposed. Then, a fuzzy system is utilized to approximate and replace the variable structure term, which can handle the unknown target acceleration. And an adaptive neural network system is adopted to compensate the effects caused by the designed overlarge acceleration of interceptor such that the interceptor with small available acceleration can intercept the high maneuvering target. Simulation results show that the guidance law with available acceleration and autopilot dynamics (AAADG) is highly effective for reducing the acceleration command and achieving a small final miss distance.

## 1. Introduction

In recent years, the hypersonic flight vehicles with high maneuverabilities have been widely developed [1]. It is necessary to design an appropriate guidance law to intercept the hypersonic flight vehicles for its high strike ability. However, the widely used PNG law [2, 3] and its variants [4–8] would fail to satisfy the requirement of high accuracy for the task of intercepting the hypersonic flight vehicles with high maneuverabilities [9]. An effective approach to intercept maneuverable targets is applying robust control methods, such as sliding mode control (SMC) [10], adaptive control [11], nonlinear $H\infty$ control [12], and optimal control [13].

The guidance law based on SMC has become an active research area because of its strong robustness and easy implementation [10, 14, 15]. In the guidance law design, the zero-effort miss distance is usually used to define sliding mode surface. For example, Shima et al. [16] proposed a sliding mode guidance law for integrated missile autopilot with the zero-effort miss distance as sliding mode surface. The sliding mode guidance laws are also designed by guiding the line-of-sight (LOS) angular rate converge to zero. Then, Zhang et al. [17] developed a novel guidance law based on integral sliding mode control and employed a nonlinear disturbance observer to estimate the target acceleration. By estimating the target acceleration via an extended state observer, Zhu et al.[18] designed a guidance law without requiring the information on the target acceleration. However, a compromise should be made between the tracking accuracy and control input since the high tracking accuracy will lead to a very large control input. Thus, the proper values for the control parameters, such as the amplitude of variable structure term, are hard to choose. Considering finite-time convergence, Zhou et al. [19] proposed a variable structure finite-time-convergent guidance law and proved that the LOS angular rate would converge to zero before the ending of the terminal guidance. To attack the target with a predefined impact angle, the guidance laws with impact angle constraints were proposed in [20–23]. Lee et al. [24] developed a guidance law using the high-

performance sliding mode control theory to intercept a stationary or slowly moving target. Kumar et al. [20] presented a guidance law to intercept the targets from any initial heading angle without exhibiting any singularity. Furthermore, some guidance laws take autopilot dynamics into consideration [25, 26]. Sun et al. [27] studied a second order sliding mode guidance law with autopilot dynamics. Li et al. [28] took both the autopilot dynamics and uncertainties into consideration and proposed a finite-time-convergent guidance law to intercept a maneuvering target.

To the best of our knowledge, the existing sliding mode guidance laws may require a greater guidance command than the available acceleration of interceptor when the maximum acceleration of target is equal to or larger than the available acceleration of interceptor. To solve this problem, an acceleration limiter is adopted to reduce the saturated acceleration demand [29, 30]. Xiong et al. [31] proposed a strategy making the coefficients of the sliding mode guidance law vary according to the fuzzy rule to reduce the acceleration demand at the beginning of the terminal guidance. However, it cannot guarantee the stability of the guidance system when the designed acceleration is significantly reduced at the end of the homing guidance. In this paper, a neural network system is employed to compensate the effects of the designed overlarge acceleration and the stability of the guidance system is proved. However, to guarantee a good performance of the guidance system when the missile intercepts the hypersonic flight vehicle with a high maneuverability, the gain of switching term needs to be chosen larger than the upper bound of target acceleration, which is hard to choose in advance and will cause the chattering problem. Then, with the universal approximation property of fuzzy systems, a continuous adaptive fuzzy system is used to approximate and replace the variable structure term, which can handle the unknown target maneuver and avoid the chattering phenomenon. The input information of the adaptive fuzzy system is the relative distance and the LOS angular rate which can be measured by the interceptor seeker easily. Besides, before designing a guidance law, it is necessary to consider the autopilot dynamics because the autopilot lag of a homing missile will decrease the precision of guidance. Then, a sliding mode guidance law considering the available acceleration and autopilot dynamics of missile for intercepting a high maneuvering target is proposed.

The main contribution of this paper is that, by adopting neural network system to reduce the acceleration command, so that the interceptor is able to intercept the hypersonic flight vehicles whose maximum acceleration is equal to or larger than the available acceleration of interceptor. In addition, the information needed to estimate the upper bound of target acceleration is limited and easy to obtain, so the proposed guidance law is easy to be implemented in practice. The rest of this paper is organized as follows. Section 2 describes the formulations of the guidance system considering the available acceleration and autopilot dynamics of interceptor. In Section 3, the control methods for the proposed guidance law are introduced. In Section 4, the stability of the guidance law is verified. At last, compared with proportional navigation guidance (PNG) and finite-time convergence guidance (FTCG), simulation results demonstrate the effectiveness of AAADG.

## 2. The Dynamics of the Relative Motion between the Interceptor and Target

This section presents the mathematic model of the guidance system for intercepting. The planar relative motion of the interceptor and target is shown in Figure 1. The interceptor and the target are denoted by the subscripts M and T, respectively. In order to simplify the guidance law design, the interceptor and target are assumed to have two mass points. The corresponding equations are given by as follows:

$$\dot{r} = -v_{\mathrm{M}}\cos\sigma_{\mathrm{M}} + v_{\mathrm{T}}\cos\sigma_{\mathrm{T}}, \tag{1}$$

$$r\dot{q} = v_{\mathrm{M}}\sin\sigma_{\mathrm{M}} - v_{\mathrm{T}}\sin\sigma_{\mathrm{T}}, \tag{2}$$

$$\sigma_{\mathrm{M}} = q - \theta_{\mathrm{M}}, \tag{3}$$

$$\sigma_{\mathrm{T}} = q - \theta_{\mathrm{T}}, \tag{4}$$

$$\dot{\theta}_{\mathrm{M}} = \frac{a_{\mathrm{M}}}{v_{\mathrm{M}}}, \tag{5}$$

$$\dot{\theta}_{\mathrm{T}} = \frac{a_{\mathrm{T}}}{v_{\mathrm{T}}}, \tag{6}$$

where $r$ is the relative distance and $\dot{r}$ is the relative velocity between the interceptor and the target. $v_{\mathrm{M}}$ is the velocity of the interceptor. $a_{\mathrm{M}}$ is the normal acceleration of the interceptor. $\theta_{\mathrm{M}}$ is the flight-path angle of the interceptor. $v_{\mathrm{T}}$ is the target velocity. $a_{\mathrm{T}}$ is the normal acceleration of the target. $\theta_{\mathrm{T}}$ is the flight-path angle of the target. $q$ and $\dot{q}$ are the light-of-sight (LOS) angle and LOS angular rate between the interceptor and target, respectively.

*Assumption 1:* [31]. In the terminal guidance, the magnitudes of the speeds of the interceptor and target are assumed as two constants such that $\dot{v}_{\mathrm{M}} = 0$ and $\dot{v}_{\mathrm{T}} = 0$.

In practice, because of the physical limitation of the interceptor actuator, the interceptor cannot achieve the required acceleration when the target acceleration is equal to or larger than the available acceleration of the interceptor. It may lead to a large final miss distance. Therefore, the required acceleration of the interceptor should be limited to a certain level. From (5), it can be seen that the acceleration of interceptor varies with the change of $\dot{\theta}_{\mathrm{M}}$. So, we can limit $\dot{\theta}_{\mathrm{M}}$ as follows:

$$\bar{\dot{\theta}}_{\mathrm{M}} = \mathrm{sat}\left(\dot{\theta}_{\mathrm{M}}\right) = \begin{cases} -\dot{\theta}_{\mathrm{M\,max}} & \dot{\theta}_{\mathrm{M}} > -\dot{\theta}_{\mathrm{M\,max}} \\ \dot{\theta}_{\mathrm{M}} & -\dot{\theta}_{\mathrm{M\,max}} \le \dot{\theta}_{\mathrm{M}} \le \dot{\theta}_{\mathrm{M\,max}} \\ \dot{\theta}_{\mathrm{M\,max}} & \dot{\theta}_{\mathrm{M}} > \dot{\theta}_{\mathrm{M\,max}} \end{cases}, \tag{7}$$

$$\bar{\dot{\theta}}_{\mathrm{M}} - \dot{\theta}_{\mathrm{M}} = \delta, \tag{8}$$

where $\dot{\theta}_{\mathrm{M\,max}} = \mathrm{const} > 0$ is the maximum flight-path angular rate of the interceptor, which is influenced by the flight environment of the interceptor, and $\bar{\dot{\theta}}_{\mathrm{M}}$ is the actual flight-path angular rate. $\delta$ is a nonlinear function caused by saturation.

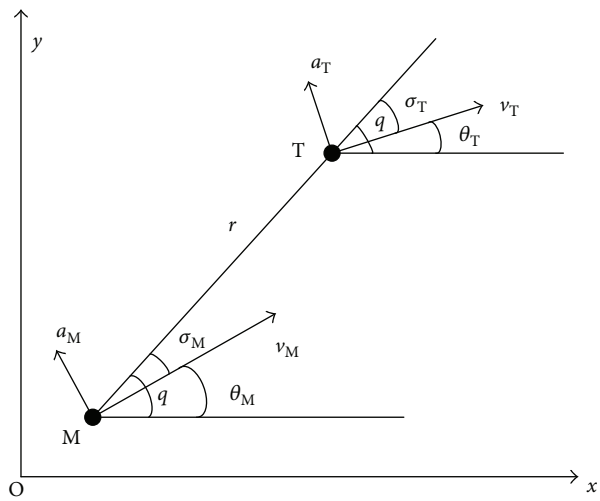


Figure 1: Relative motion between the interceptor and target.

The normal acceleration command generated by the guidance law is controlled by the autopilot of the interceptor, which tracks the expected acceleration command by modulating fins or thrusters. However, there is a lag between the expected acceleration and the achieved acceleration. Therefore, the performance of the interceptor is expected to be improved by using a guidance law considering the autopilot dynamics. The autopilot dynamics can be well modeled and approximated as the following first-order system:

$$v_M \ddot{\theta}_M = -\frac{1}{T_1} v_M \dot{\theta}_M + \frac{1}{T_1} v_M \dot{\theta}_C, \tag{9}$$

where $\dot{\theta}_C$ is the expected flight-path angular rate command of the interceptor. $\dot{\theta}_M$ is the achieved flight-path angular rate. $T_1$ is the time constant of the autopilot, which is easy to obtain in advance.

The designing purpose of the guidance law is adjusting $a_M$ so that the LOS angular rate will converge to zero. Based on this idea, we define three state variables as follows:

$$\begin{aligned} x_1 &= q, \\ x_2 &= \dot{q}, \\ x_3 &= \dot{\theta}_M. \end{aligned} \tag{10}$$

Then, we obtain the integrated dynamics equations for the guidance system with the autopilot dynamics of the interceptor as follows:

$$\begin{aligned} \dot{x}_1 &= x_2, \\ \dot{x}_2 &= -\frac{2\dot{r}}{r} x_2 - \frac{v_M \cos \sigma_M}{r} (x_3 + \delta) + \frac{1}{r} \omega, \\ \dot{x}_3 &= -\frac{1}{T_1} x_3 + \frac{1}{T_1} u, \end{aligned} \tag{11}$$

where $\omega = v_T \cos \sigma_T \dot{\theta}_T$ is the target motion information. $u$ is the actual control input.

## 3. Guidance Law Design considering Available Acceleration and Autopilot Dynamics of the Interceptor

In this section, the guidance law considering the available acceleration and autopilot dynamics of the interceptor is designed. It can be seen that the guidance system described by (11) is in a strict feedback form. However, the guidance law designed using backstepping method contains the high-order time derivatives of LOS angle and interceptor-to-target distance. To avoid this problem, the dynamic surface control method is proposed by introducing a first-order low-pass filter. The first-order low-pass filter allows the design where the model is not differentiable. For the guidance system described by (11), the goal of the guidance law is to make the LOS angular rate converge to zero. The design of the guidance law is given as follows:

$$\begin{aligned} s_1 &= x_2, \\ x_{3d} &= \frac{(k_1 + 2)|\dot{r}| x_2 + \varepsilon \operatorname{sgn} s_1 - \dot{v}_M \sin \sigma_M}{v_M \cos \sigma_M} - \hat{\delta}, \\ \frac{x_{3c}}{x_{3d}} &= \frac{1}{T_2 s + 1}, x_3(0) = x_{3c}(0), \\ s_2 &= x_3 - x_{3c}, \\ u &= x_3 + \frac{T_1}{T_2} (x_{3d} - x_{3c}) - k_2 T_1 s_2, \end{aligned} \tag{12}$$

where $s_1$ and $s_2$ are designed as the dynamic surfaces. $x_{3d}$ is the virtual control obtained from the first step. $k_1$ and $k_2$ are the dynamic surface gains. $x_{3c}$ is the command input of the second step, which is obtained by $x_{3d}$ passing through the low-pass filter. $T_2$ is the time constant of the filter. $\varepsilon$ sgn $s_1$ is the variable structure term to enhance the robustness of the system against the unknown target movement, where the switching term amplitude $\varepsilon$ satisfies $\varepsilon > |\omega|$. $\hat{\delta}$ is the adaptive acceleration compensator, which will be designed later.

*Remark 1.* The choice of the switching term amplitude $\varepsilon$ is connected to the maximum acceleration of the target. Because of the uncertain maneuver of the target, the bound of target acceleration cannot be estimated in advance. It is difficult to determine the value of switching term amplitude, since the small value of $\varepsilon$ makes the $\dot{q}$ diverge and cannot converge to zero, and the large value of $\varepsilon$ will cause heavy chattering. Moreover, as $\varepsilon$ sgn $s_1$ is not a continuous function, the interceptor actuator cannot response quickly to realize $\varepsilon$ sgn $s_1$ in practice, which will cause large miss distance.

In this paper, the adaptive fuzzy function $\hat{f}(\dot{q}, r \mid \hat{\boldsymbol{\eta}})$is chosen to approximate the switching term $\varepsilon$ sgn $s_1$. The inputs of adaptive fuzzy function are the relative distance $r$ between the interceptor and target and LOS angular rate $\dot{q}$. The switching term is replaced by the continuous function which is the output of adaptive fuzzy system, so that the improper value of $\varepsilon$ cannot influence the precision of the guidance law and the chattering phenomenon is avoided. The adaptive fuzzy system is designed as follows:

Define $b_1 = \dot{q}$ and $b_2 = r/r_0$, where $r_0$ is the initial relative distance between the interceptor and target. The knowledge based on adaptive fuzzy systems comprises a collection of fuzzy if-then rules as the following form:

(i) $R^1$: if $b_1$ is $F_1^1$ and $b_2$ is $F_2^1$, then $y$ is $G^1$.

(ii) $R^2$: if $b_2$ is $F_1^2$ and $b_2$ is $F_2^2$, then $y$ is $G^2$.

(iii) $R^3$: if $b_3$ is $F_1^3$ and $b_2$ is $F_2^3$, then $y$ is $G^3$.

(iv) $R^4$: if $b_4$ is $F_1^4$ and $b_2$ is $F_2^4$, then $y$ is $G^4$.

(v) $R^5$: if $b_5$ is $F_1^5$ and $b_2$ is $F_2^5$, then $y$ is $G^5$.

In order to approximate the switching term $\varepsilon \operatorname{sgn} s_1$ properly, the fuzzy rules should be symmetric and uniform and cover all the potential regions of $b_1$ and $b_2$. Thus, the adaptive fuzzy membership functions of the fuzzy rules in this paper are chosen as follows:

$$\begin{aligned}
u^1(b_1, b_2) &= \frac{1}{1+e^{(25b_1+1)}} \times \frac{1}{1+e^{0.5b_2}},\\
u^2(b_1, b_2) &= e^{-(5b_1+0.2)^2} \times e^{-(0.1b_2+0.2)^2},\\
u^3(b_1, b_2) &= e^{-(5b_1)^2} \times e^{-(0.1b_2)^2},\\
u^4(b_1, b_2) &= e^{-(5b_1-0.2)^2} \times e^{-(0.1b_2-0.2)^2},\\
u^5(b_1, b_2) &= \frac{1}{1+e^{(-25b_1+1)}} \times \frac{1}{1+e^{-0.5b_2}}.
\end{aligned} \tag{13}$$

Define the fuzzy basis functions as follows:

$$\xi_m(\dot{q}, r) = \frac{u^m(b_1, b_2)}{\sum_{i=1}^{5} u^i(b_1, b_2)}, \quad m = 1, 2, \dots, 5. \tag{14}$$

The switching term can be approximated and replaced by the adaptive fuzzy system. Using singleton function, center average defuzzification, and product inference, the adaptive fuzzy logic system can be expressed as follows:

$$\hat{f}(\dot{q}, r|\hat{\boldsymbol{\eta}}) = \hat{\boldsymbol{\eta}}^T \boldsymbol{\xi}(\dot{q}, r), \tag{15}$$

where $\hat{\boldsymbol{\eta}}$ is the adaptive parameter vector of the fuzzy system.

If the designed acceleration exceeds the available acceleration of interceptor too much during the terminal guidance, the control law may cause the system instable and lead to a large final miss distance. In order to solve this problem, the adaptive radial basis function neural network $\hat{\delta}$ is designed as the acceleration compensator which can compensate the influence of designed overlarge acceleration. Using the universal approximation property of neural network function, there exists an ideal neural network that approximates the nonlinear function $\delta$ in (8) closely, such that

$$\delta = \mathbf{W}^T \mathbf{h}(x_3) + \varsigma, \tag{16}$$

where $\varsigma$ is the approximation error which is very small and can be ignored. $\mathbf{W}$ is the ideal constant weight vector of neural network. And the adaptive radial basis function neural network is as follows:

$$\hat{\delta} = \hat{\mathbf{W}}^T \mathbf{h}(x_3), \tag{17}$$

where $\mathbf{h}(x_3)$ is the basis vector and $\mathbf{h}_j(x_3) = \exp(-(x_3 - c_j)^2/2b_j^2)$, $j = 1, 2, \dots, 5$. $\boldsymbol{c} = [c_1, c_2, \dots, c_5]$ is the center of the receptive field and $\mathbf{b} = [b_1, b_2, \dots, b_5]$ is the width of the Gaussian function. $\hat{\mathbf{W}}$ is the adaptive weight vector of neural network.

Neural network system is designed to compensate the influence caused by acceleration saturation of the interceptor. Therefore, the system can eliminate the limit of the available acceleration.

## 4. Stability Analysis

**Lemma 1:** [32] *Consider the system*

$$\dot{x} = g(x, t). \tag{18}$$

*Suppose that there is a continuously differentiable Lyapunov function $V(x, t)$ defined in a neighborhood of the origin. For the equation $\dot{V}(x, t) \le -\alpha V(x, t) + C$ and conditions $V(0) = p$, $\alpha > C/p$. Then, the zero solution of the system described by (18) is stable.*

**Theorem 1.** *Employing the guidance law described in (12), whose adaptive control parameters for the fuzzy system in (15) and neural network system in (17) are designed as $\dot{\hat{\boldsymbol{\eta}}} = (T_\eta r_0/r)\boldsymbol{\xi} s_1$ and $\dot{\hat{\mathbf{W}}} = -(T_W v_{\mathrm{M}} \cos \sigma_{\mathrm{M}}/r)\mathbf{h} s_1$, respectively, the guidance system described by (11) considering the available acceleration and autopilot dynamics of the interceptor is stable.*

*Proof 1.* Define the state error vector of the low-pass filter as follows:

$$\tilde{x}_3 = x_{3c} - x_{3d}. \tag{19}$$

The approximation error of the radial basis function neural network weights is defined as follows:

$$\tilde{\mathbf{W}} = \mathbf{W} - \hat{\mathbf{W}}. \tag{20}$$

Furthermore, define the optimal parameter vector $\boldsymbol{\eta}^*$ for the fuzzy system in (15) as follow:

$$\boldsymbol{\eta}^* = \arg \min_{\boldsymbol{\eta} \in \Omega} \left[ \sup_{\dot{q}, r \in \mathbb{R}} \left( \boldsymbol{\eta}^T \boldsymbol{\xi}(\dot{q}, r) - \varepsilon \operatorname{sgn} s_1 \right) \right]. \tag{21}$$

Then, the estimated error of the adaptive parameter vector for the fuzzy system is defined as follows:

$$\tilde{\boldsymbol{\eta}} = \boldsymbol{\eta}^* - \hat{\boldsymbol{\eta}}. \tag{22}$$

With the guidance law designed in (12), the time derivative of the state error vector in (19) is calculated as follows:

$$\dot{\tilde{x}}_3 = \dot{x}_{3c} - \dot{x}_{3d} = \frac{1}{T_2} x_{3d} - \frac{1}{T_2} x_{3c} - \dot{x}_{3d}. \tag{23}$$

As the optimal weight vector $\boldsymbol{\eta}^*$ of the fuzzy system in (21) and the ideal weight vector $\mathbf{W}$ of the neural network system in (16) are two constant vectors, the time derivative of

the adaptive parameter error vectors in (20) and (22) are calculated as follows:

$$\dot{\tilde{\mathbf{W}}} = -\dot{\hat{\mathbf{W}}} = \frac{T_W v_{\mathrm{M}} \cos\sigma_{\mathrm{M}}}{r} \mathbf{h} s_1, \tag{24}$$

$$\dot{\tilde{\boldsymbol{\eta}}} = -\dot{\hat{\boldsymbol{\eta}}} = -\frac{T_\eta r_0}{r} \boldsymbol{\xi} s_1. \tag{25}$$

With the guidance law designed in (12), the time derivative of $s_1$ is as follows:

$$\begin{aligned} \dot{s}_1 = &-\frac{k_1|\dot{r}|}{r} s_1 - \frac{\hat{\boldsymbol{\eta}}^T \boldsymbol{\xi}}{r} - \frac{v_{\mathrm{M}} \cos\sigma_{\mathrm{M}}}{r}\left(\delta - \hat{\delta}\right) \\ &+ \frac{1}{r}\omega - \frac{v_{\mathrm{M}} \cos\sigma_{\mathrm{M}}}{r}\left(\tilde{x}_3 + s_2\right). \end{aligned} \tag{26}$$

Similar to the process of (23), with the guidance law in (12), the time derivative of $s_2$ is calculated as follows:

$$\dot{s}_2 = -k_2 s_2. \tag{27}$$

Define the Lyapunov function candidate as follows:

$$V = \frac{1}{2}s_1^2 + \frac{1}{2}s_2^2 + \frac{1}{2}\tilde{x}_3^2 + \frac{1}{2T_\eta r_0}\tilde{\boldsymbol{\eta}}^T\tilde{\boldsymbol{\eta}} + \frac{1}{2T_W}\tilde{\mathbf{W}}^T\tilde{\mathbf{W}}, \tag{28}$$

where $T_\eta$ and $T_W$ are two positive constant. The time derivative of the Lyapunov function is computed as follows:

$$\dot{V} = s_1\dot{s}_1 + s_2\dot{s}_2 + \tilde{x}_3\dot{\tilde{x}}_3 + \frac{1}{T_\eta r_0}\tilde{\boldsymbol{\eta}}^T\dot{\tilde{\boldsymbol{\eta}}} + \frac{1}{T_W}\tilde{\mathbf{W}}^T\dot{\tilde{\mathbf{W}}}. \tag{29}$$

With the results calculated in (23), (26), and (27), it holds that

$$\begin{aligned} s_1\dot{s}_1 = &-\frac{k_1|\dot{r}|}{r}s_1^2 - \frac{\hat{\boldsymbol{\eta}}\boldsymbol{\theta}}{r}s_1 - \frac{v_{\mathrm{M}}\cos\sigma_{\mathrm{M}}}{r}\left(\delta - \hat{\delta}\right)s_1 \\ &- \frac{v_{\mathrm{M}}\cos\sigma_{\mathrm{M}}}{r}(\tilde{x}_3 + s_2)s_1 + \frac{1}{r}\omega s_1, \end{aligned} \tag{30}$$

$$s_2\dot{s}_2 = -k_2 s_2^2, \tag{31}$$

$$\begin{aligned} \tilde{x}_3\dot{\tilde{x}}_3 &= (x_{3c} - x_{3d})\left(\frac{1}{T_2}x_{3d} - \frac{1}{T_2}x_{3c} - \dot{x}_{3d}\right) \le -\frac{1}{T_2}(x_{3c} - x_{3d})^2 \\ &+ \frac{1}{2}\dot{x}_{3d}^2(x_{3d} - x_{3c})^2 + \frac{1}{2} = -\left(\frac{1}{T_2} - \frac{1}{2}\dot{x}_{3d}^2\right)\tilde{x}_3^2 + \frac{1}{2}. \end{aligned} \tag{32}$$

Substituting the results of (30), (31), and (32) into (29), the time derivative of the Lyapunov function can be reformulated as follows:

$$\begin{aligned} \dot{V} \le &-\frac{k_1|\dot{r}|}{r}s_1^2 - \frac{\hat{\boldsymbol{\eta}}\boldsymbol{\xi}}{r}s_1 - \frac{v_{\mathrm{M}}\cos\sigma_{\mathrm{M}}}{r}\left(\delta - \hat{\delta}\right)s_1 \\ &- \frac{v_{\mathrm{M}}\cos\sigma_{\mathrm{M}}}{r}(\tilde{x}_3 + s_2)s_1 + \frac{s_1}{r}\omega - k_2 s_2^2 - \left(\frac{1}{T_2} - \frac{1}{2}\dot{x}_{3d}^2\right)\tilde{x}_3^2 \\ &+ \frac{1}{2} + \frac{1}{T_\eta r_0}\tilde{\boldsymbol{\eta}}^T\dot{\tilde{\boldsymbol{\eta}}} + \frac{1}{T_W}\tilde{\mathbf{W}}^T\dot{\tilde{\mathbf{W}}} \le -\frac{k_1|\dot{r}|}{r}s_1^2 - k_2 s_2^2 \\ &- \left(\frac{1}{T_2} - \frac{1}{2}\dot{x}_{3d}^2\right)\tilde{x}_3^2 + \frac{s_1}{r}\omega - \frac{\boldsymbol{\eta}*^T\boldsymbol{\xi}}{r}s_1 \\ &+ \frac{v_{\mathrm{M}}\cos\sigma_{\mathrm{M}}}{2r}\left(\tilde{x}_3^2 + 2s_1^2 + s_2^2\right) + \tilde{\boldsymbol{\eta}}^T\left(\frac{1}{r}\boldsymbol{\xi}s_1 - \frac{1}{T_\eta r_0}\dot{\hat{\boldsymbol{\eta}}}\right) \\ &- \tilde{\mathbf{W}}^T\left(\frac{v_{\mathrm{M}}\cos\sigma_{\mathrm{M}}}{r}\mathbf{h}s_1 + \frac{1}{T_W}\dot{\hat{\mathbf{W}}}\right) + \frac{1}{2}. \end{aligned} \tag{33}$$

With the time derivatives of the estimated parameter error vectors in (24) and (25), and considering the universal approximation property of the fuzzy system as shown in (21), (33) can be rewritten as follows:

$$\begin{aligned} \dot{V} \le &-\left(\frac{k_1|\dot{r}|}{r} - \frac{v_{\mathrm{M}}\cos\sigma_{\mathrm{M}}}{r}\right)s_1^2 - \left(k_2 - \frac{v_{\mathrm{M}}\cos\sigma_{\mathrm{M}}}{2r}\right)s_2^2 \\ &- \left(\frac{1}{T_2} - \frac{1}{2}\dot{x}_{3d}^2 - \frac{v_{\mathrm{M}}\cos\sigma_{\mathrm{M}}}{2r}\right)\tilde{x}_3^2 + \frac{1}{2} + \frac{s_1}{r}\omega \\ &- \frac{\boldsymbol{\eta}*^T\boldsymbol{\xi}}{r}s_1 \le -cV + M, \end{aligned} \tag{34}$$

where $c$ and $M$ are two positive constants which satisfy the following:

$$\begin{aligned} c \le \min\Bigg(&2\left(\frac{k_1|\dot{r}|}{r} - \frac{v_{\mathrm{M}}\cos\sigma_{\mathrm{M}}}{r}\right), 2k_2 - \frac{v_{\mathrm{M}}\cos\sigma_{\mathrm{M}}}{r}, \\ &\cdot 2\left(\frac{1}{T_2} - \frac{1}{2}\dot{x}_{3d}^2 - \frac{v_{\mathrm{M}}\cos\sigma_{\mathrm{M}}}{2r}\right)\Bigg), \end{aligned} \tag{35}$$

$$M \ge \max\left(\frac{1}{2T_\eta r_0 c}\tilde{\boldsymbol{\eta}}^T\tilde{\boldsymbol{\eta}}\right) + \max\left(\frac{1}{2T_W c}\tilde{\mathbf{W}}^T\tilde{\mathbf{W}}\right) + \frac{1}{2}. \tag{36}$$

With Lemma 1, it can be concluded from (34) that the system is stable. The proof is finished.

*Remark 1.* From the guidance law designed in (12), we can get that the main parameters affecting the precisions of guidance are $k_1$, $k_2$, and $T_2$. $(k_1 + 2)$ is similar to the navigation ratio of the traditional PNG law, which is usually created from 2 to 6. And considering the choice of the constant $c$ in (35), $k_1$ can take a value from 1 to 4. According to some empirical tests, $k_2$ can be chosen from 1 to 5. $T_2$ takes a value from 0.01 to 0.5. The adaptive parameters $\hat{\mathbf{W}}$ and $\hat{\boldsymbol{\eta}}$ can be adjusted on line using the states of the interceptor and target, and their initial values are chosen as zero.

*Remark 2.* Although AAADG needs to know more information than PNG guidance law, it is not difficult to realize the

guidance law. In the proposed guidance law in (12), all the parameters needed can be measured by a target seeker easily.

*Remark 3.* Compared with the existing guidance laws, AAADG neither needs to estimate the exact maneuver information of the target nor simply treats the unknown target acceleration as zero. Meanwhile, this guidance law ensures small final miss distance under the challenging situation, where the acceleration of target is equal to or larger than the available acceleration of the interceptor.

## 5. Simulation Results

In this section, the effectiveness of AAADG is verified by numerical simulations. For the comparison purpose, we apply the proposed guidance law, the PNG and the FTCG designed in [19] to each simulation case. The proportional parameter of PNG is chosen as $k_p = 2$. The parameters of FTCG are chosen as $N = 3$, $\eta = 0.5$, $\beta = 2$, and $f = 100$. In FTCG, the sign function sgn $x$ is replaced with a saturation function $\mathrm{sat}(x)$ which is expressed as follows:

$$\mathrm{sat}(x) = \begin{cases} 1, & x > \vartheta, \\ \dfrac{x}{\vartheta}, & |x| \le \vartheta, \\ -1, & x < -\vartheta, \end{cases} \tag{37}$$

where $\vartheta$ is the small positive constant, which is chosen as 0.001 in simulation.

*Case 1.* Intercepting the target with periodic maneuver and the available acceleration of interceptor is less than the maximum acceleration of the target.

In this case, we use the proposed guidance law to intercept a target with constant velocity and sinusoidal normal acceleration. The initial position of the target is $x_{T0} = 2300$ m and $y_{T0} = 3000$ m. The initial flight-path angle is $\theta_{T0} = 0$ deg. The velocity of the target is $v_T = 1000$ m/s. And the target maneuvers with a normal acceleration is $a_T = 200 \cos t$ m/s$^2$.

The initial position of the interceptor is set as $x_{M0} = 0$ m and $y_{M0} = 0$ m, and the initial flight-path angle is $\theta_{M0} = 30$ deg. The velocity of the interceptor is $v_M = 1200$ m/s. The initial relative distance between the interceptor and target is calculated as $r_0 = 3780$ m. The initial light-of-sight angle is calculated as $q_0 = 52.5$ deg. And the available acceleration of the interceptor is 160 m/s$^2$, which is smaller than the maximum acceleration of the target. The parameters of the AAADG are chosen as $k_1 = 2$, $k_2 = 4$, $T_1 = 0.05$ s, $T_2 = 0.06$ s, $T_W = 1$, $b = [1\ 1\ 1\ 1\ 1]$, $c = [-2, -1, 0, 1, 2]$, and $T_\eta = 100$.

For Case 1, the final miss distances and impact times under three guidance laws are listed in Table 1. The accelerations of the interceptor and the LOS angle rates under three guidance laws are plotted in Figures 2 and 3, respectively. The trajectories of the interceptor and target under three guidance laws are plotted in Figure 4. The relative distances between the interceptor and target under three guidance laws are plotted in Figure 5.

Table 1: Final miss distance and impact time.

| Guidance law | PNG | FTCG | AAADG |
|---|---|---|---|
| Final miss distance (m) | 35.2539 | 8.7406 | 0.6663 |
| Impact time (s) | 13.17 | 12.97 | 12.97 |

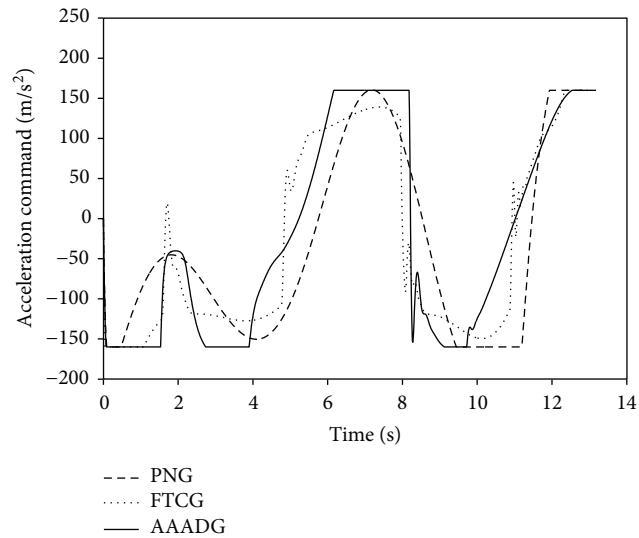


Figure 2: Accelerations under three guidance laws.

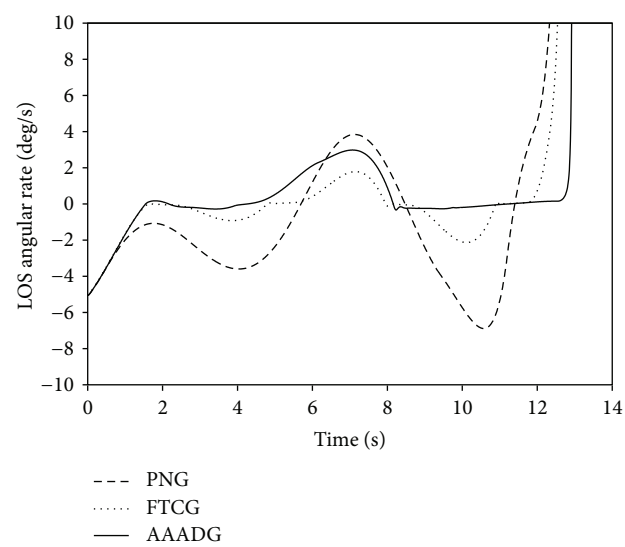


Figure 3: LOS angular rates under three guidance laws.

Figure 2 shows that the accelerations under three guidance laws are limited to 160 m/s$^2$. And at the end of the terminal guidance, the acceleration command under PNG reaches to 160 m/s$^2$ earlier than those under other two guidance laws. Moreover, from Figure 2, the acceleration commands under FTCG and AAADG reached to 160 m/s$^2$ at

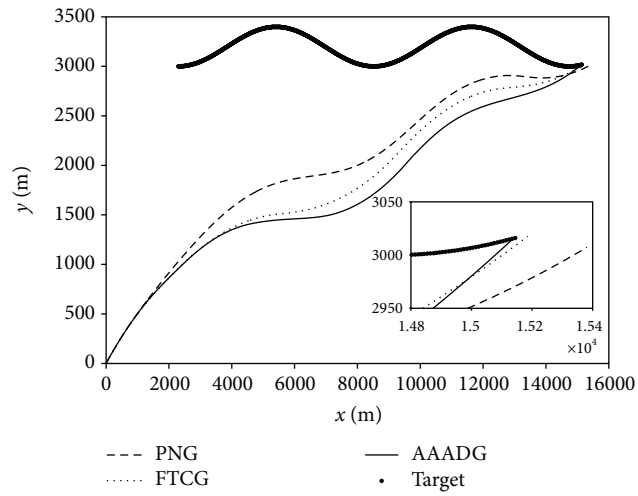


Figure 4: Trajectories of the interceptor and target under three guidance laws.

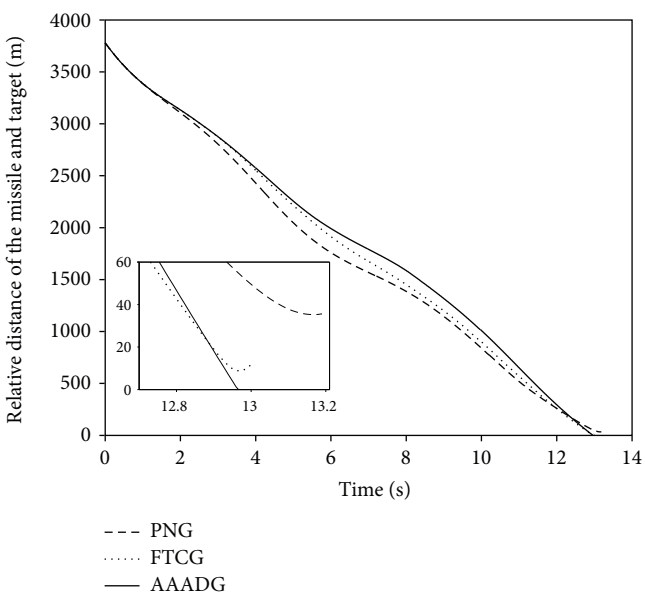


Figure 5: Relative distances between the interceptor and target under three guidance laws.

the end of the terminal guidance, but the acceleration command under FTCG has the chattering phenomenon at 11 s.

Figure 3 shows that the LOS angular rate at the beginning of the guidance is extremely large because of the initial state errors between the interceptor and target. The LOS angular rate under PNG becomes divergent too early and does not converge to zero in the terminal guidance, so the final miss distance under PNG is very large. The LOS angular rates under FTCG and AAADG converge to zero in 2 s. However, the LOS angular rate under FTCG diverges earlier than that under AAADG, such that the final miss distance under PNG is larger than that under AAADG.

Figure 4 shows the trajectories of the interceptor and target under three guidance laws. Figure 5 shows the relative

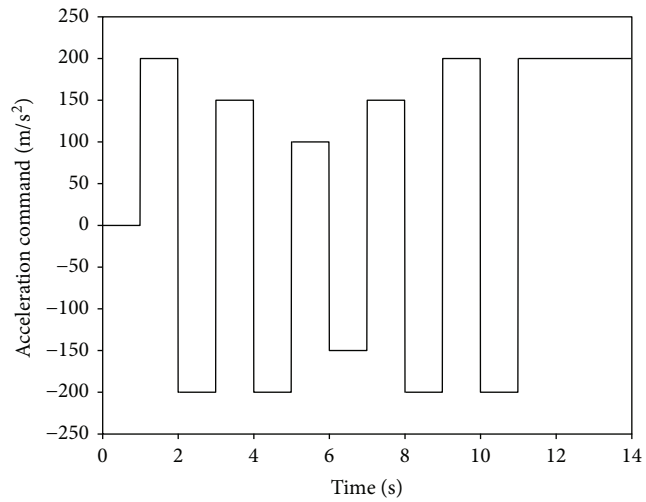


Figure 6: Target acceleration.

distance between the interceptor and target as well as the impact time. The impact time under AAADG is earlier than that under other two guidance laws, which can be seen from Figures 4 and 5 and Table 1. And the final miss distance under AAADG is the smallest.

*Case 2.* Intercepting a target with nonperiodic maneuver and the available acceleration of interceptor is equal to the maximum acceleration of the target.

In this case, the initial positions and velocities of the target and interceptor are the same as those in Case 1. The nonperiodic acceleration of the target is shown in Figure 6. The maximum acceleration of the target is 200 m/s$^2$. And the available acceleration of the interceptor is 200 m/s$^2$ which is equal to the maximum acceleration of the target.

For Case 2, the final miss distances and impact time under three guidance laws are listed in Table 2. The accelerations of the interceptor and the LOS angular rates under three guidance laws are plotted in Figures 7 and 8, respectively. The trajectories of the interceptor and target under three guidance laws are plotted in Figure 9. The relative distances between the interceptor and target under three guidance laws are plotted in Figure 10.

Figure 7 shows that the accelerations under PNG and FTCG reached to 200 m/s$^2$ too early and the acceleration under AAADG dis not reach to 200 m/s$^2$ at the end of the terminal guidance. Moreover, from Figure 8, the LOS angular rates under PNG and FTCG are divergent at the end of the terminal guidance. However, the LOS angular rate under AAADG will converge to zero at the end of the terminal guidance. Figures 9 and 10 and Table 2 show that the final miss distance under AAADG is smaller than that under other two guidance laws.

Consequently, considering the available acceleration and autopilot dynamics of the interceptor, AAADG is able to intercept the periodic and nonperiodic high maneuvering targets with small final miss distance.

Table 2: Final miss distance and impact time.

| Guidance law | PNG | FTCG | AAADG |
|---|---|---|---|
| Final miss distance (m) | 51.5315 | 42.9289 | 0.8256 |
| Impact time (s) | 13.52 | 13.44 | 13.31 |

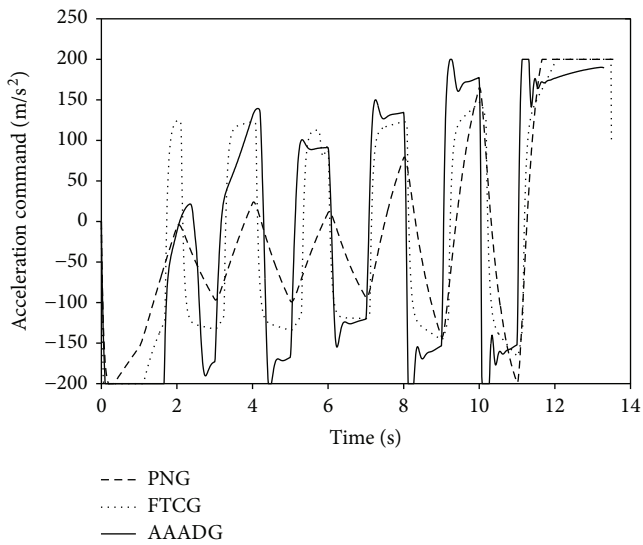


Figure 7: Accelerations under three guidance laws.

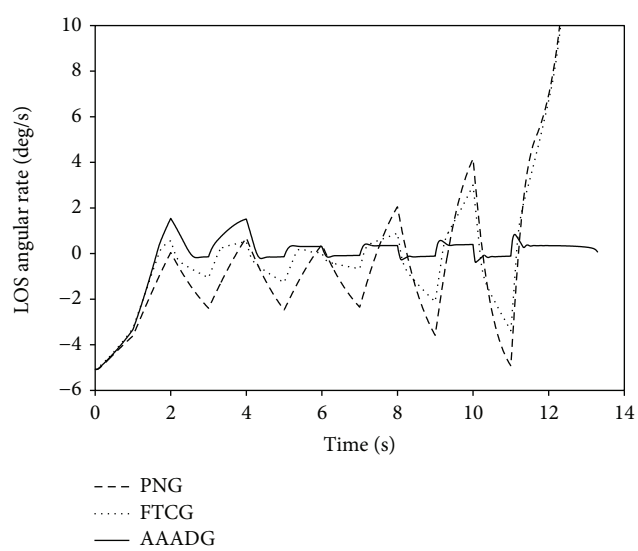


Figure 8: LOS angular rates under three guidance laws.

## 6. Conclusion

In this paper, the terminal guidance law considering the available acceleration and autopilot dynamics of the interceptor has been designed to intercept a strong maneuverable target. In the proposed guidance law, the adaptive fuzzy system is employed to approximate and replace the variable structure term, which can handle the unknown target maneuver and eliminate the chattering phenomenon.

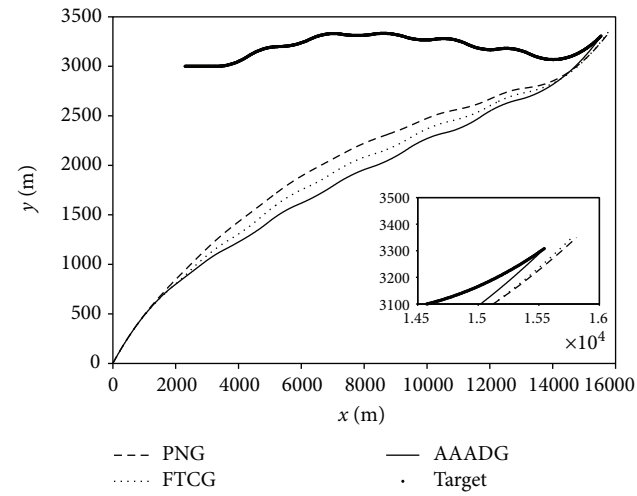


Figure 9: Trajectories of the interceptor and target under three guidance laws.

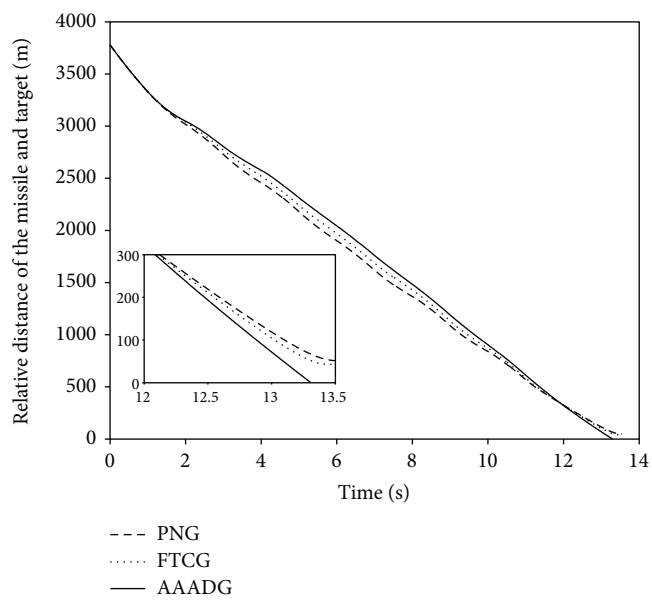


Figure 10: Relative distances between the interceptor and target under three guidance laws.

Moreover, the adaptive radial basis function neural network system is designed to compensate the influence caused by the acceleration saturation of the interceptor. Therefore, the interceptor under AAADG can intercept the hypersonic flight vehicle whose maximum acceleration is greater than or equal to the available acceleration of the interceptor. Moreover, the target information needed for AAADG is easy to obtain, so that the proposed AAADG is highly practical.

## Conflicts of Interest

The authors declare that there is no conflict of interests regarding the publication of this paper.

## Acknowledgments

This paper was sponsored by the National Natural Science Foundation of China 11202024.

## References

[1] E. N. Johnson, A. J. Calise, M. D. Curry, K. D. Mease, and J. E. Corban, "Adaptive guidance and control for autonomous hypersonic vehicles," *Journal of Guidance, Control, and Dynamics*, vol. 29, no. 3, pp. 725–737, 2006.

[2] P. J. Yuan and J. S. Chern, "Solutions of true proportional navigation for maneuvering and nonmaneuvering targets," *Journal of Guidance, Control, and Dynamics*, vol. 15, no. 1, pp. 268–271, 1992.

[3] C.-D. Yang, F.-B. Hsiao, and F.-B. Yeh, "Generalized guidance law for homing missiles," *IEEE Transactions on Aerospace and Electronic Systems*, vol. 25, no. 2, pp. 197–212, 1989.

[4] M. Guelman and J. Shinar, "Optimal guidance law in the plane," *Journal of Guidance, Control, and Dynamics*, vol. 7, no. 4, pp. 471–476, 1984.

[5] S. E. Talole and R. N. Banavar, "Proportional navigation through predictive control," *Journal of Guidance, Control, and Dynamics*, vol. 21, no. 6, pp. 1004–1006, 1998.

[6] T.-H. Kim, B.-G. Park, and M.-J. Tahk, "Bias-shaping method for biased proportional navigation with terminal-angle constraint," *Journal of Guidance, Control, and Dynamics*, vol. 36, no. 6, pp. 1810–1816, 2013.

[7] Y. A. Zhang, G. X. Ma, and H. L. Wu, "A biased proportional navigation guidance law with large impact angle constraint and the time-to-go estimation," *Proceedings of the Institution of Mechanical Engineers, Part G: Journal of Aerospace Engineering*, vol. 228, no. 10, pp. 1725–1734, 2014.

[8] B. S. Kim, J. G. Lee, and H. S. Han, "Biased PNG law for impact with angular constraint," *IEEE Transactions on Aerospace and Electronic Systems*, vol. 34, no. 1, pp. 277–288, 1998.

[9] C.-D. Yang and C.-C. Yang, "A unified approach to proportional navigation," *IEEE Transactions on Aerospace and Electronic Systems*, vol. 33, no. 2, pp. 557–567, 1997.

[10] D. Zhou, C. Mu, and W. Xu, "Adaptive sliding-mode guidance of a homing missile," *Journal of Guidance, Control, and Dynamics*, vol. 22, no. 4, pp. 589–594, 1999.

[11] D. Chwa and J. Y. Choi, "Adaptive nonlinear guidance law considering control loop dynamics," *IEEE Transactions on Aerospace and Electronic Systems*, vol. 39, no. 4, pp. 1134–1143, 2003.

[12] C. D. Yang and H. Y. Chen, "Nonlinear H robust guidance law for homing missiles," *Journal of Guidance, Control, and Dynamics*, vol. 21, no. 6, pp. 882–890, 1998.

[13] B.-G. Park, T.-H. Kim, and M.-J. Tahk, "Optimal impact angle control guidance law considering the seeker's field-of-view limits," *Proceedings of the Institution of Mechanical Engineers, Part G: Journal of Aerospace Engineering*, vol. 227, no. 8, pp. 1347–1364, 2013.

[14] J. Moon, K. Kim, and Y. Kim, "Design of missile guidance law via variable structure control," *Journal of Guidance, Control, and Dynamics*, vol. 24, no. 4, pp. 659–664, 2001.

[15] S. D. Brierley and R. Longchamp, "Application of sliding-mode control to air-air interception problem," *IEEE Transactions on Aerospace and Electronic Systems*, vol. 26, no. 2, pp. 306–325, 1990.

[16] T. Shima, M. Idan, and O. M. Golan, "Sliding–mode control for integrated missile autopilot guidance," *Journal of Guidance, Control, and Dynamics*, vol. 29, no. 2, pp. 250–260, 2006.

[17] Z. Zhang, S. Li, and S. Luo, "Terminal guidance laws of missile based on ISMC and NDOB with impact angle constraint," *Aerospace Science and Technology*, vol. 31, no. 1, pp. 30–41, 2013.

[18] Z. Zhu, D. Xu, J. Liu, and Y. Xia, "Missile guidance law based on extended state observer," *IEEE Transactions on Industrial Electronics*, vol. 60, no. 12, pp. 5882–5891, 2013.

[19] D. Zhou, S. Sun, and K. L. Teo, "Guidance laws with finite time convergence," *Journal of Guidance, Control, and Dynamics*, vol. 32, no. 6, pp. 1838–1846, 2009.

[20] S. R. Kumar, S. Rao, and D. Ghose, "Nonsingular terminal sliding mode guidance with impact angle constraints," *Journal of Guidance, Control, and Dynamics*, vol. 37, no. 4, pp. 1114–1130, 2014.

[21] Y. Zhao, Y. Sheng, and X. Liu, "Sliding mode control based guidance law with impact angle constraint," *Chinese Journal of Aeronautics*, vol. 27, no. 1, pp. 145–152, 2014.

[22] Y. Zhang, M. Sun, and Z. Chen, "Finite-time convergent guidance law with impact angle constraint based on sliding-mode control," *Nonlinear Dynamics*, vol. 70, no. 1, pp. 619–625, 2012.

[23] Z. Zhang, S. Li, and S. Luo, "Composite guidance laws based on sliding mode control with impact angle constraint and autopilot lag," *Transactions of the Institute of Measurement and Control*, vol. 35, no. 6, pp. 764–776, 2013.

[24] C.-H. Lee, T.-H. Kim, and M.-J. Tahk, "Design of impact angle control guidance laws via high-performance sliding mode control," *Proceedings of the Institution of Mechanical Engineers, Part G: Journal of Aerospace Engineering*, vol. 227, no. 2, pp. 235–253, 2013.

[25] P. Qu and D. Zhou, "A dimension reduction observer-based guidance law accounting for dynamics of missile autopilot," *Proceedings of the Institution of Mechanical Engineers, Part G: Journal of Aerospace Engineering*, vol. 227, no. 7, pp. 1114–1121, 2013.

[26] S. S. Moosapour, G. Alizadeh, S. Khanmohammadi, and H. Moosapour, "A novel robust proportional navigation guidance law design for missile considering autopilot dynamic," *Transactions of the Institute of Measurement and Control*, vol. 35, no. 5, pp. 703–710, 2013.

[27] S. Sun, D. Zhou, and W. Hou, "A guidance law with finite time convergence accounting for autopilot lag," *Aerospace Science and Technology*, vol. 25, no. 1, pp. 132–137, 2013.

[28] G.-L. Li, H. Yan, and H.-B. Ji, "A guidance law with finite time convergence considering autopilot dynamics and uncertainties," *International Journal of Control Automation and Systems*, vol. 12, no. 5, pp. 1011–1017, 2014.

[29] W. Wang, S. Xiong, X. Liu, S. Wang, and L. Ma, "Adaptive nonsingular terminal sliding mode guidance law against maneuvering targets with impact angle constraint," *Proceedings of the Institution of Mechanical Engineers, Part G: Journal of Aerospace Engineering*, vol. 229, no. 5, pp. 867–890, 2014.

[30] C.-M. Lin and C.-F. Hsu, "Guidance law design by adaptive fuzzy sliding-mode control," *Journal of Guidance, Control, and Dynamics*, vol. 25, no. 2, pp. 248–256, 2002.

[31] J. H. Xiong, S. J. Tang, J. Guo, and T. N. Wang, "Improved sliding mode guidance law based on fuzzy variable coefficients strategy," *The Aeronautical Journal*, vol. 118, no. 1202, pp. 435–451, 2014.

[32] M. Hou, X. Liang, and G. Duan, "Adaptive block dynamic surface control for integrated missile guidance and autopilot," *Chinese Journal of Aeronautics*, vol. 26, no. 3, pp. 741–750, 2013.

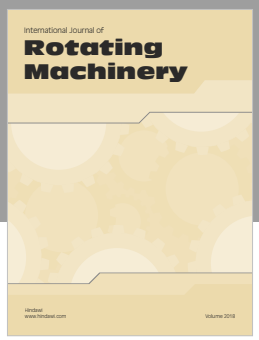

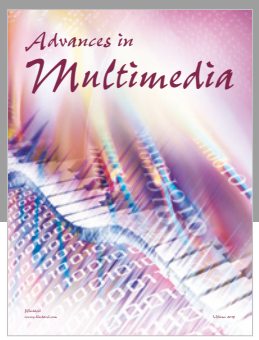

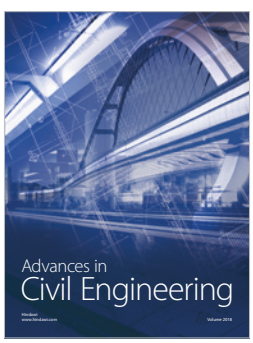

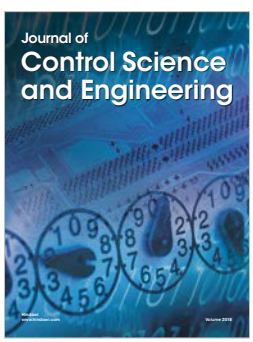

Hindawi
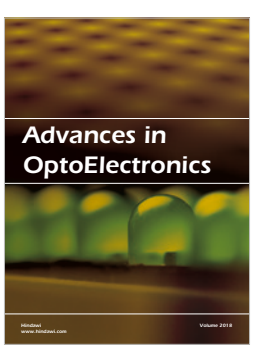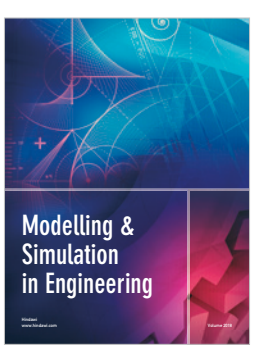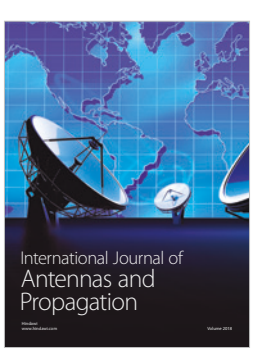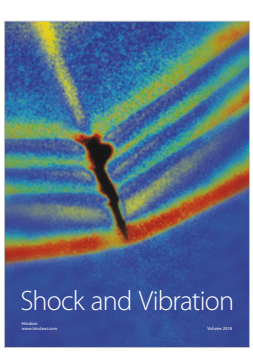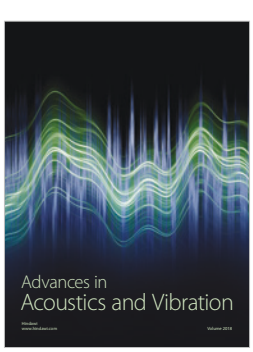
Submit your manuscripts at
www.hindawi.com